Analysis of power scintillation and fading margin in the LEO-ground downlink with the OSIRISv1 laser terminal on Flying Laptop and the DLR Optical Ground Station Oberpfaffenhofen

Florian Moll*[a], Dirk Giggenbach[a], Christopher Schmidt[a], Christian Fuchs[a]
[a]DLR Institute of Communications and Navigation, Oberpfaffenhofen, 82234 Wessling, Germany

ABSTRACT

Free-space optical communications is an emerging field for a variety of use cases in the domain of satellite communications. It is deployed in Earth observation missions to downlink payload data, in telecom missions (GEO or LEO based) to up- and downlink data streams and in quantum communication missions to implement the needed quantum and classical channels. Part of the propagation path goes through the atmosphere where the propagating optical wave experiences wave-front distortions and consequently distortions of the irradiance field. These distortions lead to scintillation of the optical power in the focal plane of the optical ground stations receiver front-end which can cause signal outages. Characterization of power scintillation is very important to assess the needed fading margin in the communication link design. Thus, these power scintillations are matter of investigation in this paper. Measurement campaigns were conducted to experimentally characterize the power scintillation. Received power was measured with a 40 cm telescope located at the DLR site Oberpfaffenhofen, i.e. in a suburban area. Satellite source is the OSIRISv1 laser terminal on the LEO satellite Flying Laptop. The campaigns were conducted in the years 2018, 2019 and 2020 where data of 15 passes could successfully be recorded. The power scintillation statistics are analyzed over elevation. The power scintillation index shows different behavior from pass to pass which is due to the different environmental conditions during the individual passes. Median values and quartiles of power scintillation index over elevation are given. Furthermore, statistics of fading margin for link budget calculation are derived. Both can be used to define best, nominal and worst cases in the design of the LEO-ground communication link.

Keywords: free-space optical communications, satellite communications, scintillation, optical turbulence, channel modelling, Flying Laptop, OSIRISv1, fading margin

1. INTRODUCTION

Free-space optical satellite communications is an emerging field which is entering commercial markets. Use cases are, for example, Earth observation missions, telecom networks and quantum networks [1][2]. The first addresses the need to downlink a big amount of data generated by the space borne sensor to Earth. The link in this case is unidirectional, i.e. in downlink direction only. The second case deals with establishing satellite-based telecom networks (or network branches) which involves bi-directional links between satellite and from satellites to ground. The third case deals with supplying the public or classical channel which is needed for the implementation of quantum communication protocols, e.g. quantum key distribution. In all these use cases, part of the propagation path goes through the atmosphere. Whilst propagating, the phase of the optical wave is distorted and the resulting self-interference of the beam causes the intensity profile to turn into a speckle pattern which changes in time. This phenomenon is called intensity scintillation. The intensity field is received by a telescope and focused onto a received front-end. Thus, the signal is converted into an optical power which fluctuates over time. This phenomenon is called power scintillation. Characterization of this power scintillation is very important since it causes fading of the data communication signal. In this work, we focus on the downlink direction which is important for all mentioned use cases.

*florian.moll@dlr.de; phone +49 8153 28-2876; dlr.de

PREPRINT

The central statistical parameter for characterization of the power scintillation is the power scintillation index (PSI), σ_p^2 [-], as defined by equation 1, where P_{Rx} [W] is the received optical power [6].

$$\sigma_p^2 = \frac{\left\langle P_{Rx}^2 \right\rangle - \left\langle P_{Rx} \right\rangle^2}{\left\langle P_{Rx} \right\rangle^2}. \quad (1)$$

Goal of this work is to give figures of the PSI over elevation and to show the dynamics of the parameters that can occur in a real mission, i.e. show the variability over different satellite passes. Theoretical models existed that enable calculation of PSI based on an assumed turbulence profile [3][4][5][6]. However, many assumptions are included in this modelling. Therefore, measurements are used in this work to characterize the PSI. Furthermore, the PSI can be used to calculate fading loss which is an important parameter in the link budget calculation.

The paper is structured as follows: chapter 1 gives the motivation and introduction into the topic. Chapter 2 describes the measurement setup which was used to acquire time series of received power. This includes the space source and the ground station setup. In chapter 3, we describe the conducted measurement campaign and the resulting data base. The method of data analysis is given in chapter 4. The measurement results and an example usage of it for fading loss calculation is given in chapter 5. Discussion, conclusion and outlook are done in chapter 6.

2. MEASUREMT SETUP

2.1 General

The measurements setup comprises the space source and the ground station as measurement device. The ground station follows the satellite during the satellite pass and light is coupled onto the individual sensors, specifically a power sensor in this data analysis.

2.2 Space source

The used space source for these power scintillation measurements is the OSIRISv1 laser communication terminal onboard the Flying Laptop satellite (FLP) [7]. The laser beam steering is based on satellite body pointing without any optical feedback by uplink beacon from ground. The AOCS (Attitude and Orbit Control System) of the satellite uses star cameras and fiber-optic gyroscope as sensors. The remaining error in orientation to the optical ground station is compensated by a beam divergence of 1.2 mrad (full beam divergence) with an optical transmit power of 1 W in the range of 1550 nm. The satellite was launched into low Earth orbit with of 586 x 604 km and 97.5° inclination on 14th July 2017 and has been used in several laser downlink experiments till now. The satellite and the integrated laser terminal module are shown in Figure 1.

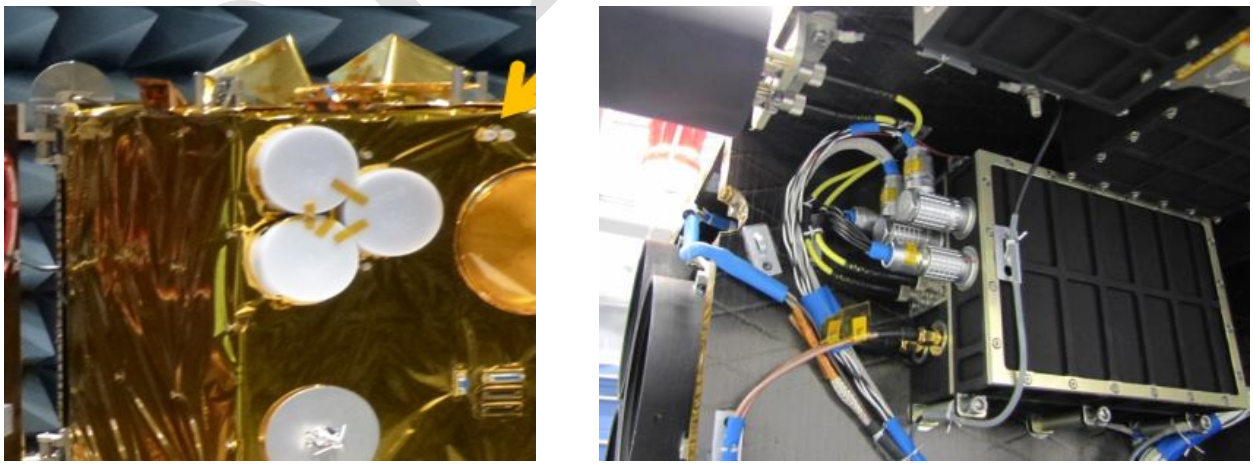

Figure 1. Flying Laptop Satellite with marked position of the OSIRISv1 transmit collimators (left). OSIRISv1 module as integrated in the satellite (right). Image credit: University of Stuttgart.

PREPRINT

2.3 Ground station

The used ground station is DLR`s Optical Ground Station Oberpfaffenhofen. It is located on the DLR site Oberpfaffenhofen nearby Munich, Germany, in 600 m height asl [8]. The central instruments of the station are the Cassegrain telescope with 40 cm main mirror diameter, the clamshell dome and the optical backplane (Figure 2). The last hosts the power meter instrumentation. It comprises a beam collimation optics and a PIN diode which signal is sampled at 20 kHz rate.

Figure 2. Telescope and dome of Optical Ground Station Oberpfaffenhofen (left). Optical backplane with power sensor installed (right). Image credit: DLR.

3. MEASUREMENT CAMPAIGN

Downlink experiment were carried out in the years 2019 and 2020 on a regular basis to first, test the satellite payload, and second, acquire measurements of power scintillation data. Measurements from 15 satellite passes contain good data for power scintillation analysis. Meta data of the 15 measurements are given in Table 1.

Table 1. Overview of optical downlink experiments

OSIRISv1 trial #	**Date**	**Start of pass (UTC)**	**Max elevation**
O118-01	20.09.18	22:50	62°
O118-02	25.09.18	22:02	42°
O118-03	25.09.18	23:38	22°
O119-01	17.04.19	21:02	18°
O119-02	17.04.19	22:27	50°
O119-03	18.04.19	21:12	22°
O119-04	18.04.19	22:47	40°
O119-05	19.04.19	21:21	27°
O119-06	24.04.19	22:09	83°
O119-07	01.05.19	21:40	42°
O119-08	01.05.19	23:16	22°
O119-09	05.06.19	20:50	15°
O119-10	05.06.19	22:25	60°

PREPRINT

OSIRISv1 trial #	Date	Start of pass (UTC)	Max elevation
O119-11	08.06.19	21:21	27°
O119-12	29.06.19	21:26	35°

4. DATA ANALYSIS

Careful data analysis was performed to eliminate all sources of potential error. For example, since Flying Laptop uses no uplink beacon as reference, beam pointing jitter is relatively large compared to the beam divergence. This causes significant low frequency modulation of the received scintillation signal which has strong impact on the power scintillation index. Therefore, occasions where beam jitter changes PSI must be detected and removed.

An overview of the analysis steps is given in Figure 3.The *Execute* block contains the subdivisions *Select trial and data channel*, *Define analysis parameters* and *Set paths and file names*. The block *Select trial and data channel* selects the individual trials from the different measurement campaigns and years as well as the data channel, i.e. the power meter behind the 40 cm telescope and the power meter behind the 5 cm telescope (several instruments were used in the measurements campaign). The block *Define analysis parameters* contains the definition of thresholds for minimum interval time, signal-to-noise ratio (SNR) and saturation and intervals of excluded measurements. Sliding window size is set and optics parameters are given. Furthermore, definition of auto-correlation time and fade statistics are set. The block *Set paths and file names* contains the definition of the folder and file structure for source and result data.

The *Preprocessing* block contains the subdivisions *Extract data*, *Filter data*, *Identify valid data*, *Remove offset*, *Correct for pass dynamics* and *Correct for beam slew*, The block *Extract data* loads the measurement raw data together with the data of the orbital information. Viewing direction of the telescope and range to the satellite are calculated and time synchronized with the measurement data. The block *Filter data* comprises the definition of a suitable low pass filter and the deployment of the filter. The block *Identify valid data* detects valid data samples based on definition of SNR, saturation and excluded measurement intervals. Furthermore, it maps time and elevation vectors. The block *Remove offset* calculates the offset due to background and noise signals and performs subtraction from the measurement signal. Furthermore, it removes influence of the filter wheel. The block *Correct for pass dynamics* includes the correction for change in free-space loss and in atmospheric transmission. Last, the block *Correct for beam slew* identifies the data intervals where low frequency mis-pointing had impact on the measurement results and removes it.

The *Parameter calculation* block contains the subdivisions *Power scintillation index*, *Correlation time*, *Probability density function*, *Fade statistics* and *Spectrum*. These individual blocks contain calculation of the respective parameters.

The *Post-processing* block contains the subdivision *Create passes statistics*, *Save data* and *Plot graphs*. The block *Create passes statistics* calculates the median and quantiles over the analyzed satellites passes. The block *Save data* stores the data on hard drive. The block *Plot graphs* creates plots of the calculated parameters over time and elevation.

The block *Plausibility-check* includes the *Evaluation against expectation* and *Exclusion of failed data*. This means, that when a plausibility check is negative, the data processing is either repeated with adopted analysis parameters (e.g. concerned data intervals are removed).

PREPRINT

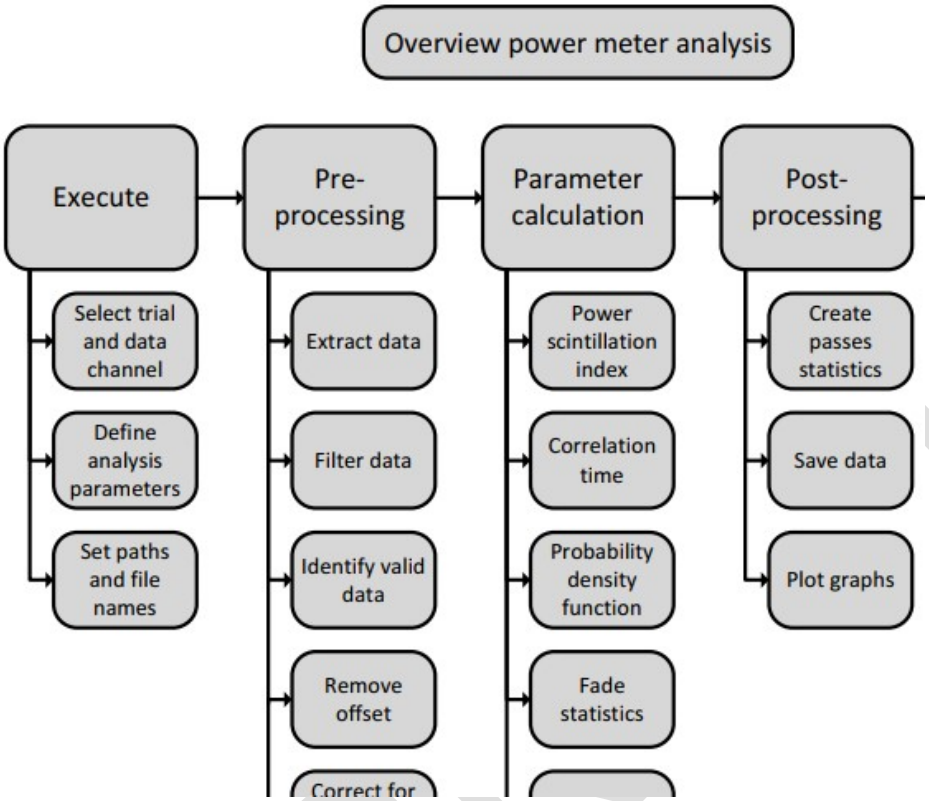

Figure 3. Overview of power meter analysis.

5. MEASUREMENT RESULTS

5.1 PSI measurements overview

Figure 4 (top) shows the PSI over elevation for a single satellite pass (O118-01, 22.09.2018, 22:50). PSI is maximum around 2-4 deg elevation and decreases with increasing elevation angle. Saturation of scintillation can be observed at the low elevations. This is presumably due to increasingly smaller speckle sizes, aperture averaging increases and thus PSI decreases.

The results for all analyzed passes are given in Figure 4 (bottom). A strong variability of PSI over the different passes is visible which indicates different atmospheric conditions. For example, a spreading of values of factor 10 at 20 deg elevation is observed which is the maximum spread for these passes. This spread is smaller for other elevations, especially for lower ones. Reason might be start of saturation at very low elevations, e.g. below 10 deg. A different reason might the behavior of single passes. Pass O118-02 shows high PSI over the whole elevation range which contributes a lot to the PSI spread at 20 deg elevation.

PREPRINT

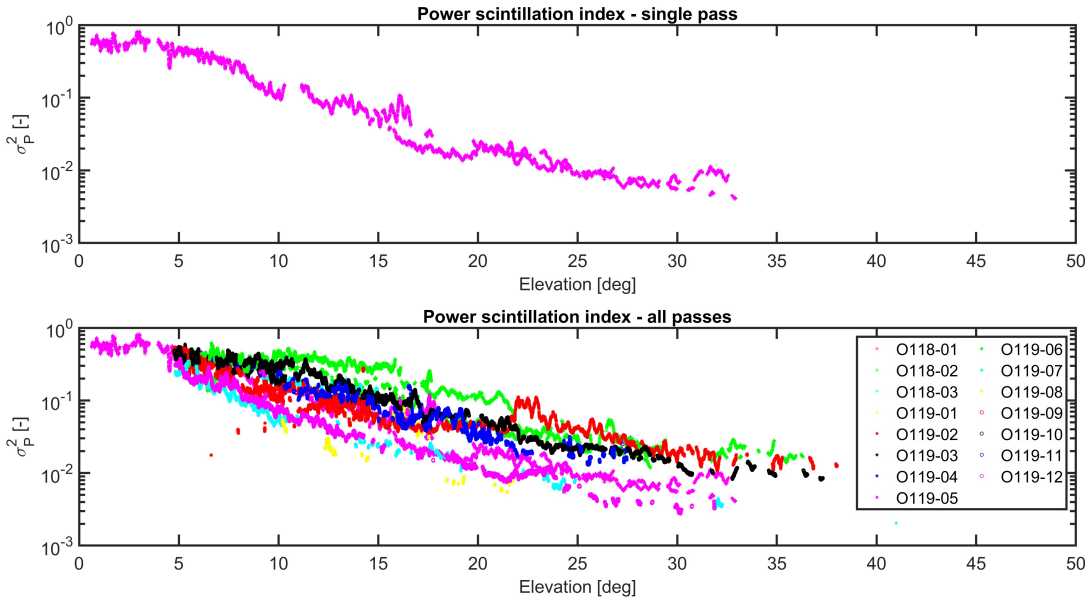

Figure 4. Overview of PSI of all analyzed satellite passes. The upper figure shows a single satellite pass for better visualization, while the lower figure shows the lines for all analyzed passes.

Median values and quantiles are calculated and shown in Figure 5. The broken lines above 35 deg elevation are due to lack of measurement in this region. The dark grey area contains 50% of all analyzed cases. The bright grey area (including the dark area) contain 80 % of all analyzed cases. Values above 30 deg elevation are expected to monotonously decrease further due to less atmospheric volume traversed. Instead, a local increase at 35 deg can be observed. Reason may be the lack of data in this region.

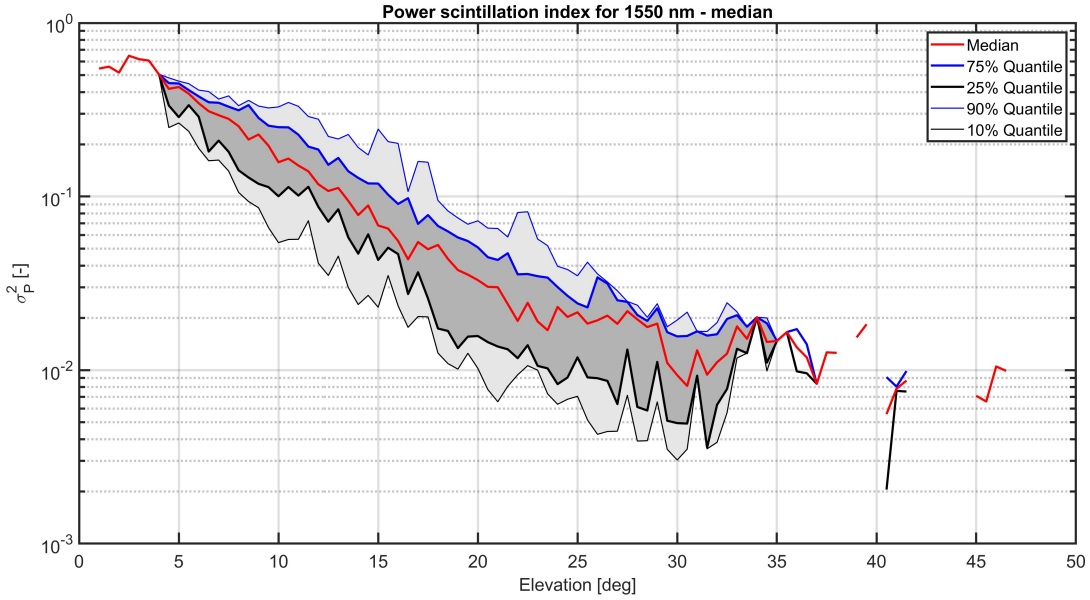

Figure 5. Median of power scintillation index with quantiles. Data above 35 deg elevation is sparse and thus the lines are broken.

5.2 Fading margin statistics

Link feasibility is usually analyzed with link budget calculation. Here one important parameter is the fading margin (or fading loss) that is used to take into account scintillation of the received power on the data receiver. Assuming that all bits are lost when the signal drops below the specified receiver sensitivity (minimum optical power), the fading margin a_{sci}, with power scintillation index σ_p^2 can be calculated according to [9]

$$a_{sci} = 4.3\left\{\mathrm{erf}^{-1}(2p_{thr}-1)\cdot\left[2\ln(\sigma_p^2+1)\right]^{1/2} - \tfrac{1}{2}\ln(\sigma_p^2+1)\right\}. \quad (2)$$

The power threshold p_{thr} gives the allowed fractional fading time. Equation 2 uses a threshold approach which means that a certain acceptable time fraction is defined, during which the received power is below a minimum acceptable power. The required power margin between the average received power and the minimal received power is seen as a loss (fading margin) which can be considered in link budget calculation. It is important to note that this link budget calculation is in optical domain only. This means that specification of receiver sensitivity must be in optical power. If electrical power is considered, the dependency between optical and electrical power must be considered which is linear for PIN type receivers (thermal-noise limited) but root-shaped for APD type receivers (shot-noise limited) [11].

The median of this fading loss with quantiles taking as input the PSI values from Figure 5 is given in Figure 6. The run of the fading loss over elevation equals the run of the PSI due to the approximately linear relation. To give some numerical examples, we have a look at 10 deg elevation. Fading loss at the lower bound (10 % quantile) is 2.4 dB, median value is 4.2 dB and upper bound (90 % quantile) is 6.0 dB. This results in a dynamic of 4.2±1.8 dB. At 20 deg elevation we have 1.9±0.9 dB.

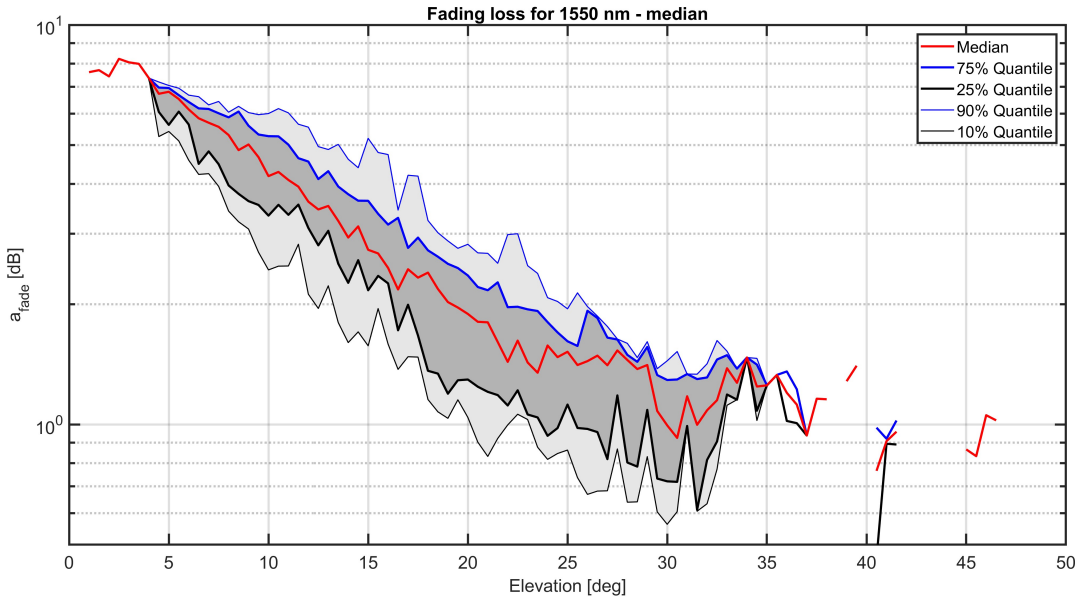

Figure 6. Median of fading margin with quantiles. Time fraction for fade threshold is taken as p_{thr} = 0.01. Data above 35 deg elevation is sparse and thus the lines are broken.

6. SUMMARY AND OUTLOOK

Analysis of power scintillation data from 15 satellite passes is presented and statistics of PSI over elevation in terms of median and quantiles is given. Data below 5 deg and above 30 deg elevation is sparse and therefore, interpretation of these regions must be especially careful. Saturation of scintillation can be observed at low elevations but this needs to be confirmed with further measurements. PSI spread is observed to vary for different elevation, e.g. for 20 deg elevation it is a factor of about 10 but smaller for lower and higher elevations.

The statistics of PSI are used to calculate statistics of fading margin which again can be used in link budget calculation to define nominal, worst, and best cases. The presented method to calculate fading margin is rather conservative since it assumes that no data can be detected during fades, i.e. the channel is modelled by on/off states as done in [9] and [10]. For use of the PSI values from Figure 6 in fade margin/link budget calculations, the sensitivity of the receiver must be given in optical power since relation between optical and electrical power may be between linear to root, depending on the type of receiver used.
Further work is needed for consolidation and improvement of the results. E.g. a focus on measurements at elevations higher than 35° and lower than 5° and in total increase of the statistical basis is needed. Another aspect is, for instance, the validation of the measurement results against expectations from theoretical analysis. In addition, the current analysis method can be further improved. At the moment, measurements intervals with strong slopes of received power due to satellite jitter are detected and excluded from the analysis. A more sophisticated approach would be spectral filtering of the low frequency jitter.

The next research step (aside improving the current results) is using the PSI and fading margin results in a more detailed fading analysis which includes also the calculation of fade length and fade frequency. For this, an analysis of the observed quasi-frequency will also be needed.

ACKNOWLEDGEMENTS

The project on which this report is based was partially funded by the German Federal Ministry of Education and Research under the funding code 16KIS1079 and 16KIS1265. The authors are responsible for the content of this publication. Furthermore, the authors give thanks to the Flying Laptop team of University of Stuttgart for operating the satellite.

REFERENCES

[1] A. K. Majumdar, “Laser Communication with Constellation Satellites, UAVs, HAPs and Balloons”, Springer International Publishing, 2022.
[2] J. S. Sidhu et al., “Advances in space quantum communications”, IET Quantum Communication , Vol. 2, No. 4, p. 182-217, 2021.
[3] L. C. Andrews, “Aperture-averaging factor for optical scintillations of plane and spherical waves in the atmosphere” , J. Opt. Soc. Am. , Vol. 9, No. 4, p. 597-600, 1992.
[4] J. H. Churnside, “Aperture averaging of optical scintillations in the turbulent atmosphere”, Appl. Opt. , Vol. 30, No. 15, p. 1982-1994, 1991.
[5] H. T. Yura, W. G. McKinley, “Aperture averaging of scintilllation for space-to-ground optical communication applications”, Applied Optics, Vol. 22, No. 11, p. 1608-1609, 1983.
[6] L. C. Andrews, R. L. Philips, “Laser Beam Propagation through Random Media”, 2nd. Edition, SPIE Press: Belligham, 2005.
[7] J. Keim, S. Gaißer, P. Hagel, M. Böttcher, M. Lengowski, M. Graß, D. Giggenbach, C. Fuchs, C. Schmidt, S. Klinkner, “Commissioning of the Optical Communication Downlink System OSIRISv1 on the University Small Satellite Flying Laptop”, 70th International Astronautical Congress (IAC), Washington, Oct. 2019.
[8] F. Moll, A. Shrestha, C. Fuchs, “Ground stations for aeronautical and space laser communications at German Aerospace Center”, Proc. of SPIE 9647, 2015.
[9] D. Giggenbach, H. Henniger, “Fading-loss assessment in atmospheric freespace optical communication links with on-off keying”, Opt. Eng., Vol. 47, No. 4, 2008.
[10] D. Giggenbach, Dirk, F. Moll, “Scintillation Loss in Optical Low Earth Orbit Data Downlinks with Avalanche Photodiode Receivers”, Proc. of ICSOS 2017, IEEE Xplore, 2017.
[11] D. Giggenbach, R. Mata-Calvo, Sensitivity Modeling of Binary Optical Receivers”, Applied Optics, Vol. 54, No. 28, October 1, 2015.

PREPRINT